PHOTOMASK

BACUS—The international technical group of SPIE dedicated to the advancement of photomask technology.

BACUS
N • E • W • S

MARCH 2019
VOLUME 35, ISSUE 3

Photronics Best Student Oral Paper — PUV18

Measurement and Modeling of Diffusion Characteristics in EUV Resist

Luke Long and Andrew Neureuther, University of California, Berkeley, United States
Patrick Naulleau, Lawrence Berkeley National Laboratory, United States

Abstract

As a critical driver of the resolution, line edge roughness, sensitivity trade-off, understanding acid diffusion in chemically amplified resist (CAR) is critical for its continued use in extreme ultraviolet lithography. Here we present an experiment that probes the nature of acid diffusion in a commercially available, conventional polymer CAR by measuring the developed linewidth of features as a function of post exposure baketime. In contrast to deep ultraviolet resists, the linewidth vs baketime relationship in the EUV resist studied is not linear. The observed trend in EUV was shown to be well described by the multivariate Poisson propagation model using a Gaussian diffusion kernel with a diffusivity of 25 nm^2/s. Deviations from a purely Gaussian diffusion profile were modeled by the inclusion of base that reduces the effective acid concentration in unexposed regions of resist. We thus conclude that acid blur in EUV CAR can be well described as a Fickian diffusion process.

1. Introduction

A major development in the history of photolithography was the introduction of chemically amplified photoresist (CAR). In these resists, electromagnetic information from the mask is discretely transferred into acid information within the resist through the interaction of light and photoacid generators (PAGs). In turn, these acids catalytically react with their polymer host during post exposure bake (PEB) to “deprotect” the polymer side chains, allowing the patterning of the resist by exploiting changes in resist solubility caused by the reaction. The diffusion of photoacid plays two key and coupled roles in this process: 1) In allowing the acid to move spatially, acid diffusion facilitates the amplification of the photon image by allowing multiple deprotection reactions per acid. 2) In producing an effective volume surrounding each photoacid generation site, acid diffusion allows for the smoothing of the photon and chemical

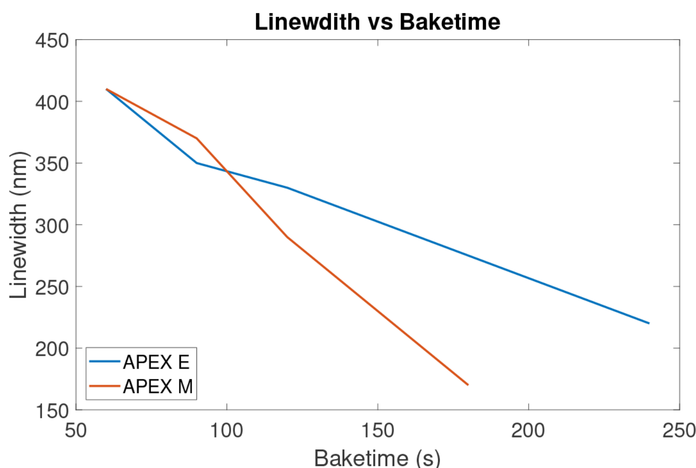

Figure 1. Linewidth vs Baketime Data for DUV Resist. Zuniga, SPIE 1994[1].

TAKE A LOOK INSIDE:

INDUSTRY BRIEFS
—see page 6

CALENDAR
For a list of meetings
—see page 7

SPIE.

10809-10

EDITORIAL

Freestyle chess, machine learning, and new paradigms for computational patterning

D.N. Dunn, IBM Research

Much has been made of how recent advances in hardware have enabled an explosion of machine learning algorithms and applications to problems in science and technology. One exciting aspect of research in this area has been the development of augmented intelligence paradigms. In these paradigms, teams of engineers work in tandem with advanced machine learning tools to solve problems more effectively than either using engineers or computers alone. A good illustration of this approach can be found in the unexpected freestyle chess tournament victory by two relative amateurs at the 2005 computer-assisted PAL/CSS Freestyle Chess Tournament (News, 2005). One of the interesting questions posed by freestyle chess is whether teams of human players working with assistance from machines can beat sophisticated computer only systems? The answer to this question was a resounding yes in the PAL/CSS Freestyle Chess Tournament in which three grand masters had eliminated all but one team by the final round. The interesting aspect of the final round is that a grand master team, working with help from computers, was facing a team of relative new comers who were also using machines, but all the machine-only competition had been eliminated handily. More importantly, the new comers beat the grand master team by a significant margin (News, 2005).

At this point, you may be asking yourself, what does a demonstration of the power of humanmachine teaming from nearly 14 years ago have to do with computational patterning? The answer to this question is straightforward. With the explosion of interest in the application of machine learning to technical problems, there have been a lot of task specific demonstrations showing how different types of machine learning algorithms can be used to detect lithographic hotspots (Yibo Lin, 2017), place subresolution assist features (Shibing Wang, 2017), (Yibo Lin, 2017), and apply optical proximity correction (Tetsuaki Matsunawa, 2016), (Xu Ma, 2014). Results presented in these papers and others show impressive gains in both run-time and accuracy over traditional methods. These results are significant in and of themselves, but one of the key areas of criticism for these methodologies is what happens when things go wrong i.e. when a hotspot is not a hotspot or measured errors on wafer are significantly higher than predicted? How do engineering teams triage results and implement fixes in a timely fashion? At first glance these questions may be interpreted as significant obstacles, but we believe that they represent unprecedented opportunities to develop augmented intelligence flows that tackle some of the most difficult problems facing computational patterning.

One area that we find particularly exciting is how machine learning techniques in hotspot detection and OPC can be applied early in design technology co-optimization (DTCO) to quantitatively assess the probability of success for candidate design styles and ground rules. As was pointed out in a previous editorial (Dunn, 2017), we are constantly looking for ways to capture the impact of downstream biases in DTCO simulation flows to identify design constructs that correctly capture the full entitlement of patterning and mask processes to deliver robust design rules that are aggressive but maximize production process windows. Machines are proficient at objectively identifying hotspots, but experienced engineers are adept at recognizing whether a hotspot is truly a hotspot and identifying probable fixes.

Another area that presents additional opportunity to leverage augmented intelligence flows is to define methods using traditional simulation and mask generation tools to improve the accuracy of training algorithms as well as to supplement inference. Significant gains can be realized by leveraging source optimization and inverse lithography techniques to improve the accuracy and guidance of machine learning algorithms by computational patterning teams. In addition, traditional empirical bias modeling methodologies can be applied to capture mask processes where necessary in to augmented intelligence approaches to DTCO, OPC, and hotspot flows.

While it is easy to recognize an opportunity as valuable, it is far more difficult to implement flows that fully leverage these opportunities. There is still a lot of work to be done to develop flows and methodologies that leverage the best of machine learning, traditional simulation flows, and engineering intuition with necessary run-time efficiency and accuracy to deliver new technology nodes. We are looking forward to participating and contributing to this new area and welcome others to participate in delivering industry leading solutions that leverage augmented intelligence flows.

N • E • W • S

ˆBACUS News is published monthly by SPIE for BACUS, the international technical group of SPIE dedicated to the advancement of photomask technology.

Managing Editor/Graphics Linda DeLano

SPIE Sales Representative, Exhibitions, and Sponsorships Melissa Farlow

BACUS Technical Group Manager Marilyn Gorsuch

■ **2019 BACUS Steering Committee** ■

President
Peter D. Buck, *Mentor Graphics Corp.*

Vice-President
Emily E. Gallagher, *imec*

Secretary
Kent Nakagawa, *Toppan Photomasks, Inc.*

Newsletter Editor
Artur Balasinski, *Cypress Semiconductor Corp.*

2019 Annual Photomask Conference Chairs
Jed Rankin, *GLOBALFOUNDERIES Inc.*
Moshe Preil, *KLA-Tencor Corp.*

International Chair
Uwe F. W. Behringer, *UBC Microelectronics*

Education Chair
Frank E. Abboud, *Intel Corp.*

Members at Large
Michael D. Archuletta, *RAVE LLC*
Brian Cha, *Samsung Electronics Co., Ltd.*
Derren Dunn, *IBM Corp.*
Thomas B. Faure, *GLOBALFOUNDRIES Inc.*
Aki Fujimura, *DS2, Inc.*
Brian J. Grenon, *Grenon Consulting*
Jon Haines, *Micron Technology Inc.*
Naoya Hayashi, *Dai Nippon Printing Co., Ltd.*
Bryan S. Kasprowicz, *Photronics, Inc.*
Patrick M. Martin, *Applied Materials, Inc.*
Jan Hendrik Peters, *bmbg consult*
Stephen P. Renwick, *Nikon Research Corp. of America*
Douglas J. Resnick, *Canon Nanotechnologies, Inc.*
Thomas Scheruebl, *Carl Zeiss SMT GmbH*
Thomas Struck, *Infineon Technologies AG*
Bala Thumma, *Synopsys, Inc.*
Anthony Vacca, *Automated Visual Inspection*
Michael Watt, *Shin-Etsu MicroSi Inc.*
Larry Zurbrick, *Keysight Technologies, Inc.*

SPIE.

P.O. Box 10, Bellingham, WA 98227-0010 USA
Tel: +1 360 676 3290
Fax: +1 360 647 1445
SPIE.org
help@spie.org

©2019

All rights reserved.

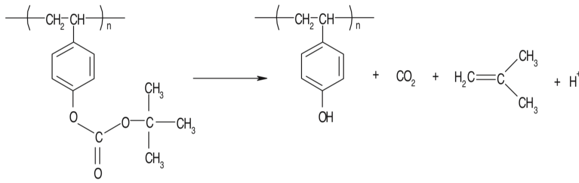

Figure 2. Simple model of tBoc deprotection mechanism[3].

noise inherent to lithographic processes due to the quantum nature of light and matter. As the high energy nature of EUV photons leads to a decrease in the number of photons per unit dose, understanding acid diffusion phenomena becomes even more important as projection lithography transitions to the use of 13.5 nm light.

The prototypical model for acid diffusion is given by Fick's law, which states that the rate of change of the concentration of a chemical species is given by the negative divergence of the flux at each point in space.

Mathematically, this can be expressed as

$$\frac{\partial \rho}{\partial t} = \nabla \cdot (D(x,t)\nabla \rho). \tag{1}$$

In the event that the diffusivity, $D(x,t)$, is spatially constant, this equation can be written

$$\frac{\partial \rho}{\partial t} = D(t)\Delta \rho. \tag{2}$$

Furthermore, if the diffusivity is a constant in time as well, then the solution to this partial differential equation takes the form of a Gaussian point spread function (PSF). This allows concentrations to be determined for all space and time by the convolution of the PSF with the initial concentration distribution:

$$\rho(t) = \left(\frac{1}{\sqrt{4\pi Dt}} exp[\frac{-x^2}{4Dt}]\right) * \rho(x,0). \tag{3}$$

From a probabilistic perspective, the Gaussian kernel can be thought of as describing a sphere of radius = $\sqrt{2Dt}$ that the initial acid distribution at each point in space effectively occupies after diffusing for a time t. In so far as the availability of acid is the limiting factor in the deprotection of the photoresist, this suggests that a "deprotection front" will travel through the resist such that the relationship between the critical dimension (CD) of an exposed line will change during PEB by an amount proportional to $\sqrt{t}$. Hereafter this relationship will be referred to as "Fickian" diffusion, while deviations attributable to concentration and deprotection-dependent diffusivities that serve to accelerate or retard the spread of acid will be referred to as "non-Fickian."

Table 1. Table of values used in MPPM.

Parameter	Value
PAG	$0.2/nm^3$
Base	Varable
D_{Acid}	$25nm^2/s$
D_{Base}	$0nm^2/s$
k_{ab}	$10nm^3/s$
$k_{deprotection}$	$1nm^3/s$
QE	2.08
electron blur	$2nm$
absorptivity	$4.3/\mu m$

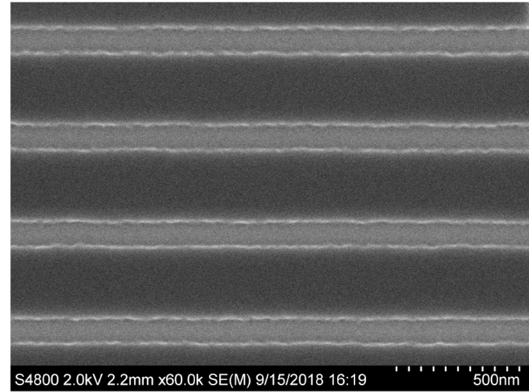

Figure 3. Example SEM Image. This particular image corresponds to a 60s baketime.

Evidence for non-Fickian diffusion has been reported for DUV resists[1], where a linear CD vs baketime relationship was observed. This deviation from Fickian behavior was hypothesized to be due to a dynamically changing, spatially varying diffusivity within the resist. Mechanistically, these deviations could be due to a change in free volume within the resist as the deprotection proceeds; an increase in free volume provides more space for photoacid to move, thus increasing the mobility of the acid within the resist, while a decrease in free volume has the opposite effect. To explain the relationship between deprotection and free volume, consider the tBOC mechanism shown in Figure 2. As a by product of the reaction, two volatile chemicals are produced, which are known to outgas during PEB. The voids left behind by these chemical species would naturally lead to an overall increase in free volume. Competing against this effect is that the deprotection reaction and outgassing destabilize the mechanical structure of the resist. This is known to lead to resist shrinkage as high as 30%[2]. Either of these mechanisms would lead to a diffusivity that is variable in both time and space, and would necessitate the usage of Equation 1 to properly model the acid diffusion characteristics.

The purpose of the new work presented in this paper was to examine the acid diffusion characteristics of CAR that are currently used for EUV exposure. Since the data presented by Zuniga et al., much has changed about CAR. For one, the thickness of the resist has shrunk from around half a micron for the APEX resists to 45 nm for the resist studied here. Additionally, progress has been made on the use of quencher to reduce the local acid concentration in unexposed regions of resist. This paper studies the ability of a Fickian diffusion model to describe a CD vs baketime experiment in a typical EUV CAR.

2. Experimental

2.1 Wafer Preparation

A commercially available, conventional polymer CAR was studied. The exposed wafers were coated with HDMS in order to promote photoresist adhesion. Resist thickness was measured to be 45 nm using a NanoSpec 6100 automated film thickness measurement system.

2.2 Exposure

Wafers were exposed using an electron beam writing tool. The accelerating voltage was 100keV corresponding to a backscatter range of $\approx$ 31 μm. The full width half max of the electron beam was 8 nm. Electron beam exposure was chosen as it allows for very sharp exposure profiles. Electron beam exposure provides a good analog to the radiation chemistry that drives EUV exposure. Furthermore, in terms of deposited energy per unit volume, electron beam exposure has

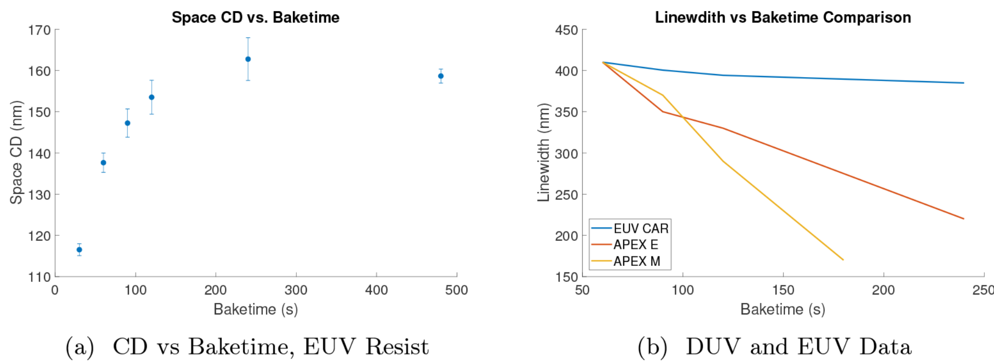

(a) CD vs Baketime, EUV Resist (b) DUV and EUV Data

Figure 4. Experimental Data.

been shown to be comparable to EUV[4]. The exposed lines were 100 nm wide with 300nm of unexposed resist in between. This pitch was chosen to allow plenty of room between lines for acid diffusion, and to avoid mutual diffusion between lines.

2.3 Post Exposure Bake & Development

Following exposure, wafers were baked for 30, 60, 90, 120, 240, and 480s. Sixty seconds is the nominal baketime of the resist. Baketimes were thus chosen to cover a broad range of factors of the nominal baketime, from 50% to 8x, allowing for a full characterization of the effect of baketime on acid diffusion.

2.4 Feature Analysis

Features were imaged with a Hitachi S-4800 SEM. For each baketime, the line space pattern was imaged in five different locations. SEM images were analyzed using SuMMIT. The average width of exposed was measured at each baketime. Reported CDs are the average of the measured CDs from each image, with error bars given by the standard deviation of the five measurements. An example SEM image can be found in Figure 3.

2.5 Modeling

To model the reaction diffusion process during PEB, the multivariate Poisson propagation model (MPPM) was used. In short, the MPPM populates model cells with photons/electrons and molecules according to a Poisson distribution, with means given by the average dose and chemical loadings respectively. More details about the model can be found in the references[5][6]. Of importance to this paper is the nature of reaction diffusion equations used in this model:

$$\frac{\partial \rho_{acid}}{\partial t} = D_{acid}\,\Delta\,\rho - k_{ab}\rho_{acid}\,\rho_{base} \tag{4}$$

$$\frac{\partial \rho_{base}}{\partial t} = D_{base}\,\Delta\,\rho - k_{ab}\rho_{acid}\,\rho_{base} \tag{5}$$

$$\frac{\partial \rho_{deprotection}}{\partial t} = k_{deprotection}\,\rho_{acid}\,(1 - \rho_{deprotection}) \tag{6}$$

The first terms of Equations 4 and 5 refer to a Fickian diffusion term for the acid and base, respectively, while the second term corresponds to an annihilation reaction between the acid and the base. Equation 6 describes the deprotection rate, whose rate is proportional to the acid concentration times the “protection” concentration, where deprotection/protection are defined to be numbers between 0 and 1 corresponding to how reacted/unreacted the polymer is in a given location. A list of model values can be found in Table 1.

3. Results

The results of the experiment are shown in Figure 4a, and plotted next to the DUV CAR data in 4b. The first notable feature is that, in contrast to the DUV resist, the data shows a decided non-linear CD vs baketime relationship. Additionally, the overall change in the linewidth during PEB is much less for the EUV resist than for DUV, consistent with the ability of modern resist to pattern features >10x smaller than in 1994.

However, the relationship is not well described by a simple $\sqrt{t}$ relationship, either, as the CD rolls off in time more rapidly that predicted by pure diffusion. In order to explain this effect the impact of quencher on the linewidth vs baketime relationship was modeled. With a diffusivity of $25 nm^2/s$, the quencher concentration could be tuned such that the CD is well matched at each of the measured baketimes. As evidenced by the curves in Figure 5, a base loading of 0:08 $molecules/nm^3$, or 40% of the PAG loading, fit the data well. The MPPM model shows a strong impact of quencher on the deprotection characteristics of the resist. Specifically, the more quencher is added, the more dramatic the flattening of the CD vs baketime curve. This highlights the expected importance of quencher in controlling the deprotection reaction[7] despite its stochastic costs[8].

4. Conclusions

The linewidth vs baketime study conducted suggests that diffusion characteristics in EUV CAR differ from those in their DUV counterparts. As opposed to a linear relationship found in the DUV resist, the EUV CAR showed linewidth vs baketime data more closely resembling a $\sqrt{t}$ functional form. However, the acid diffusion is slowed compared to a simple Fickian diffusion profile. This effect was adequately modeled with a Gaussian diffusion kernel and an acid quencher annihilation reaction iteratively applied in the MPPM model. This suggests that modern resist is not strongly affected by dynamic, concentration or deprotection-dependent changes in diffusivity during PEB.

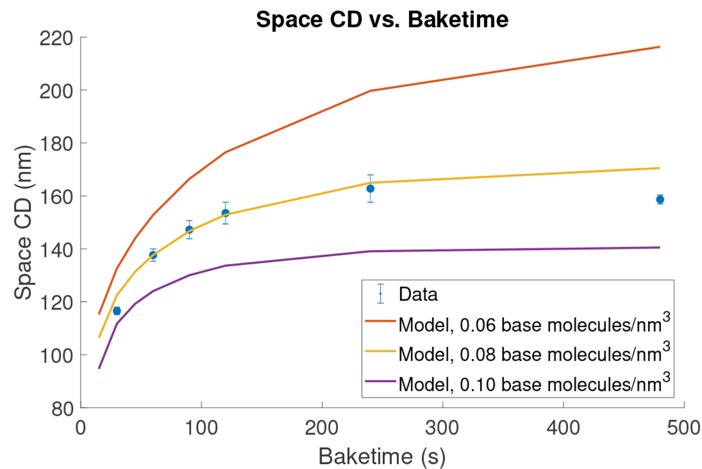

Figure 5. Experimental data with model curves. Model curves correspond to different quencher loadings. PAG loading was 0.2 molecules/nm³.

5. References

[1] M. Zuniga, E. Tomacruz, and R. Neureuther, "Diffusion Effects in Chemically Amplified Deep-UV Resists," **Proc. of SPIE 2195** (May 1994), pp. 320–328, 1994.

[2] G. M. Waliraff, W. D. Hinsberg, F. A. Houle, M. Morrison, C. E. Larson, M. Sanchez, P. J. Brock, G. Breyta, H. Road, S. Jose, G. Wallraff, W. D. Hinsberg, F. A. Houle, M. Morrison, C. E. Larson, M. Sanchez, J. Hoffnagle, P. J. Brock, and G. Breyta, "Experimental method for quantifying acid diffusion in chemically amplified resists," **Proc. of SPIE 3678** (June 1999), p. 138, 1999.

[3] E. Reichmanis, "Chemical amplification mechanism for microlithography," *Polymeric Materials Science and Engineering, Proceedings of the ACS Division of Polymeric Materials Science and Engineering 66*, 1992.

[4] S. Bhattarai, A. R. Neureuther, and P. P. Naulleau, "Study of shot noise in photoresists for extreme ultraviolet lithography through comparative analysis of line edge roughness in electron beam and extreme ultraviolet lithography," *Journal of Vacuum Science & Technology B, Nanotechnology and Microelectronics: Materials, Processing, Measurement, and Phenomena 35*(6), p. 061602, 2017.

[5] G. M. Gallatin, "Resist blur and line edge roughness," Optical Microlithography XVIII, Pts 1-3 5754 (May 2004), pp. 38–52, 2005.

[6] P. P. Naulleau and G. M. Gallatin, "Effect of resist on the transfer of line-edge roughness spatial metrics from mask to wafer," *Journal of Vacuum Science & Technology B, Nanotechnology and Microelectronics: Materials, Processing, Measurement, and Phenomena 28*(6), pp. 1259–1266, 2010.

[7] K. Asakawa, T. Ushirogouchi, and M. Nakase, "Effect of remaining solvent on sensitivity, diffusion of acid, and resolution in chemical amplification resists," *Journal of Vacuum Science & Technology B 13*(3), p. 833, 1995.

[8] P. Naulleau, C. Anderson, W. Chao, S. Bhattarai, and A. Neureuther, "Stochastics and EUV Patterning in the 1x-nm Regime," *Journal of Photopolymer Science and Technology 29*(6), pp. 797–802, 2016.

BACUS N • E • W • S

Sponsorship Opportunities

Sign up now for the best sponsorship opportunities

Photomask Technology + EUV Lithography 2019

Contact: Melissa Farlow, Tel: +1 360 685 5596; melissaf@spie.org

Advanced Lithography 2019

Contact: Teresa Roles-Meier, Tel: +1 360 685 5445; teresar@spie.org

Advertise in the BACUS News!

The BACUS Newsletter is the premier publication serving the photomask industry. For information on how to advertise, contact:

Melissa Farlow,
Tel: +1 360 685 5596
melissaf@spie.org

BACUS Corporate Members

Acuphase Inc.
American Coating Technologies LLC
AMETEK Precitech, Inc.
Berliner Glas KGaA Herbert Kubatz GmbH & Co.
FUJIFILM Electronic Materials U.S.A., Inc.
Gudeng Precision Industrial Co., Ltd.
Halocarbon Products
HamaTech APE GmbH & Co. KG
Hitachi High Technologies America, Inc.
JEOL USA Inc.
Mentor Graphics Corp.
Molecular Imprints, Inc.
Panavision Federal Systems, LLC
Profilocolore Srl
Raytheon ELCAN Optical Technologies
XYALIS

Industry Briefs

Global Semiconductor Sales Increase 13.7% to $468.8B in 2018

The Semiconductor Industry Association (SIA), representing U.S. leadership in semiconductor manufacturing, design, and research, today announced the global semiconductor industry posted sales of $468.8 billion in 2018, the industry's highest-ever annual total and an increase of 13.7 percent compared to the 2017 total. Global sales for the month of December 2018 reached $38.2 billion, a slight increase of 0.6 percent over the December 2017 total, but down 7.0 percent compared to the total from November 2018. Fourth-quarter sales of $114.7 billion were 0.6 percent higher than the total from the fourth quarter of 2017, but 8.2 percent less than the third quarter of 2018.

https://electroiq.com/2019/02/global-semiconductor-sales-increase-13-7-to-468-8b-in-2018/

Multi-Beam Litho Shakeout

The multi-beam e-beam market for lithography applications continues to undergo a shakeout amid technical roadblocks and other issues.

Last week, ASML announced that it had acquired the intellectual-property (IP) assets of Mapper Lithography, a Dutch supplier of multi-beam e-beam tools for lithography applications that fell into bankruptcy late last year. As it turns out, ASML will not continue to develop Mapper's multi-beam lithography technology, according to the company. Mapper's R&D employees, who will join ASML, will work on various projects at ASML.

Generally, the e-beam market can be divided into two main segments—photomask and lithography. E-beam technology is alive and well on the photomask front. For years, photomask makers have used single-beam e-beam systems to write patterns on a mask.

NuFlare is the leader in the single-beam mask writer market. Then, IMS, a subsidiary of Intel, sells a multi-beam e-beam tool for photomask writing. IMS' technology works and is making masks today. NuFlare is working on multi-beam mask writer technology as well.

https://semiengineering.com/manufacturing-bits-feb-5/

Current Challenges and New Frontiers for EUV

The 2018 Source Workshop was held in November in Prague, co-organized with HiLASE. Among the highlights from the workshop was ASML's presentation of progress in EUV source and EUVL scanner. The latest version of the scanner currently has 246 W source with 80% availability to support 140 wafers per hour (WPH) throughput. It was pointed out that the reason for downturn is the long mean time to repair (MTTR). Pellicle transmission is now at 83%, with a goal of 90%.

EUV source power is now feasible at 450 W (3% duty cycle and 15 ms bursts). Such sources will provide additional power for the next generation of EUVL scanner at 0.3 NA. However, power requirements for the 0.5 NA scanner are yet not clear, and also we lack clarity on how well traditional Sn LPP will support power requirements between 500 – 1000 W. Free-electron laser (FEL) sources technology is an option, but so far we do not have experimental results on which to base our opinions.

Metrology sources for EUVL are getting ready to support high volume manufacturing (HVM) level mask metrology tools. The brightness, long term stability, power and cost of ownership need to improve to support 5 nm node tool specifications.

http://electroiq.com/euvl-focus/2019/02/07/current-challenges-and-new-frontiers-for-euv-sources-update-from-2018-source-workshop/

Join the premier professional organization for mask makers and mask users!

About the BACUS Group

Founded in 1980 by a group of chrome blank users wanting a single voice to interact with suppliers, BACUS has grown to become the largest and most widely known forum for the exchange of technical information of interest to photomask and reticle makers. BACUS joined SPIE in January of 1991 to expand the exchange of information with mask makers around the world.

The group sponsors an informative monthly meeting and newsletter, BACUS News. The BACUS annual Photomask Technology Symposium covers photomask technology, photomask processes, lithography, materials and resists, phase shift masks, inspection and repair, metrology, and quality and manufacturing management.

Individual Membership Benefits include:

- Subscription to BACUS News (monthly)
- Eligibility to hold office on BACUS Steering Committee

spie.org/bacushome

Corporate Membership Benefits include:

- 3-10 Voting Members in the SPIE General Membership, depending on tier level
- Subscription to BACUS News (monthly)
- One online SPIE Journal Subscription
- Listed as a Corporate Member in the BACUS Monthly Newsletter

spie.org/bacushome

CALENDAR

2019

Photomask Japan
16-18 April 2019
PACIFICO Yokohama
Yokohama, Japan
photomask-japan.org

The 35th European Mask and Lithography Conference, EMLC 2019
17-19 June 2019
Hilton Hotel Dresden
Dresden, Germany

SPIE Photomask Technology + EUV Lithography
15-19 September 2019
Monterey Conference Center and
Monterey Marriott
Monterey, California, USA

2020

SPIE Advanced Lithography
23-27 February 2020
San Jose Marriott and
San Jose Convention Center
San Jose, California, USA

SPIE is the international society for optics and photonics, an educational not-for-profit organization founded in 1955 to advance light-based science, engineering, and technology. The Society serves nearly 264,000 constituents from 166 countries, offering conferences and their published proceedings, continuing education, books, journals, and the SPIE Digital Library in support of interdisciplinary information exchange, professional networking, and patent precedent. SPIE provided more than $4 million in support of education and outreach programs in 2018. **spie.org**

SPIE.
International Headquarters
P.O. Box 10, Bellingham, WA 98227-0010 USA
Tel: +1 360 676 3290
Fax: +1 360 647 1445
help@spie.org • **spie.org**

Shipping Address
1000 20th St., Bellingham, WA 98225-6705 USA

Managed by SPIE Europe
2 Alexandra Gate, Ffordd Pengam, Cardiff,
CF24 2SA, UK
Tel: +44 29 2089 4747
Fax: +44 29 2089 4750
spieeurope@spieeurope.org • **spieeurope.org**

You are invited to submit events of interest for this calendar. Please send to lindad@spie.org; alternatively, email or fax to SPIE.